Iranian Journal of Materials Forming 13 (4) (2026) 24-33

IJMF

Online ISSN: 2383-0042

Iranian Journal of Materials Forming

Journal Homepage: http://ijmf.shirazu.ac.ir

Research Article

The Effect of Cyclic Closed Die Forging (CCDF) Process on Fatigue Crack Growth Behavior of Precipitation-Hardened Al 7075 Alloy

Mohammad Ali Moazam and Mohammad Honarpisheh*

Faculty of Mechanical Engineering, University of Kashan, Kashan, Iran

ARTICLE INFO

Article history:

Received: 28 January 2026
Reviewed: 15 April 2026
Revised: 30 April 2026
Accepted: 9 May 2026

Keywords:

Aluminum alloy 7075
Cyclic closed die forging (CCDF)
Fatigue crack growth
Crack growth rate (da/dN)
Stress intensity factor range (ΔK)

Please cite this article as:

Moazam, M. A. & Honarpisheh, M. (2026). The effect of cyclic closed die forging (CCDF) process on fatigue crack growth behavior of precipitation-hardened Al 7075 alloy. *Iranian Journal of Materials Forming*, *13*(4), 24-33. https://doi.org/10.22099/ijmf.2026.55549.1371

ABSTRACT

In this study, the effect of the cyclic closed die forging (CCDF) process on the fatigue crack growth rate (da/dN) of aluminum alloy 7075 in the peak-aged (T6) condition was experimentally investigated. Specimens were prepared in three different conditions: base T6, T6 with one pass of CCDF, and T6 with two passes of CCDF. Fatigue crack growth tests were conducted in accordance with the ISO 12108 standard using compact tension (CT) specimens. Key parameters, including the stress intensity factor range (ΔK) and crack growth rate (da/dN), were calculated and compared. The results indicated that CCDF-processed specimens exhibited about 33% improvement in resistance to fatigue crack initiation. They also tolerated more than 1 mm greater fatigue crack growth compared to the T6 specimen. Finally, the crack growth rate of CCDF-processed specimens decreased by up to 18% compared to the T6 specimen. Furthermore, no significant difference was observed between the performance of specimens subjected to one pass and two passes of CCDF. This improvement can be attributed to the refined microstructure, increased dislocation density, and better distribution of precipitates resulting from the CCDF process. The findings of this research represent an effective step towards optimizing hybrid processes for improving the fatigue life of aluminum components in engineering applications.

© Shiraz University, Shiraz, Iran, 2026

1. Introduction

7000-series aluminum alloys, particularly aluminum 7075, are widely used in aerospace, automotive, and fatigue-loaded structural applications due to their high strength-to-weight ratio and favorable mechanical properties. However, the susceptibility of these alloys to fatigue crack initiation and growth under cyclic loading remains a major challenge in the design of critical components, necessitating methods to improve fatigue crack growth resistance.

Severe plastic deformation (SPD) processes are recognized as effective methods for modifying microstructure and enhancing the mechanical properties of materials. Among these, the cyclic closed die forging

* Corresponding author
E-mail address: honarpishe@kashanu.ac.ir (M. Honarpisheh)
https://doi.org/10.22099/ijmf.2026.55549.1371

Published by Shiraz University. This is an open access article under the CC BY-NC-ND license (http://creativecommons.org/licenses/by-nc-nd/4.0/).

(CCDF) process has attracted significant attention due to its ability to induce high, uniform deformation without introducing surface cracks. This process, by applying high strain, leads to grain refinement and increased dislocation density, which can potentially influence the material's fatigue behavior.

Gosh [1] first utilized the CCDF method in 1988 to produce an ultra-fine-grained structure in aluminum alloys. In that study, by presenting a thermomechanical process and using the aforementioned CCDF method, it was stated that a superplastic ultra-fine-grained aluminum could be produced, achieving a specific uniaxial tensile elongation exceeding 1270%. Cherukuri and Srinivasan in 2006 [2] studied the hardness and mechanical properties of AA6061 alloy under the CCDF process, also known as multi-axial compression/forging (MAC/F). They reported that microhardness across the cross-section was non-uniform in both as-received and first-pass processed samples, and uniform hardness distribution was achieved with an increased number of passes. Zude et al. [3] in 2010 investigated the microstructure and mechanical properties of AM60B magnesium alloy. The results of this research indicated that with increasing total applied strain during the CCDF process, the grain size decreased and the mechanical properties improved. Gao et al. [4] in 2012 deformed AZ80 alloy via the CCDF method and studied its microstructure and mechanical properties. They showed that the yield strength, ultimate tensile strength, and elongation of the CCDF-processed AZ80 alloy improved by 89%, 45%, and 242%, respectively, compared to its as-cast state. Xia et al. [5] in 2013 studied the microstructure and mechanical properties of AZ61 alloy in the CCDF process. They described the mechanism of ultra-fine grain formation in the studied alloy and, besides improving mechanical properties, managed to reduce the grain size from 152 μm to approximately 16.5 μm. Metayer et al. [6] in 2014 studied the microstructure, mechanical, and wear properties of several Mg-Si family alloys before and after CCDF treatment. In this study, the size of precipitating intermetallic particles was investigated using XRD, and the obtained results indicated that the size of these particles decreased due to the CCDF process.

On the other hand, precipitation hardening heat treatment (Age Hardening) to achieve the T6 condition is a common method for increasing yield and ultimate strength in aluminum alloys. However, the combined effects of this heat treatment with severe plastic deformation processes on fatigue behavior, particularly the fatigue crack growth rate (da/dN), are not yet fully understood. Investigating these synergistic effects can provide strategies for achieving materials with an optimal balance between strength and fracture toughness.

Previous studies have primarily focused on examining the separate effects of SPD processes or heat treatments on static properties or initial fatigue behavior (crack initiation). For example, research has shown that processes like ECAP and HPT can increase fatigue crack initiation resistance in aluminum alloys [7, 8]. Also, T6 heat treatment leads to the formation of fine, strengthening precipitates that significantly increase strength [9, 10]. However, the simultaneous impact of these two methods on crack growth mechanisms and key parameters such as stress intensity factor range (ΔK) and its relationship with da/dN requires further experimental investigation.

Sha et al. [11] studied the fatigue behavior and crack growth rate in Al7075 alloy after the cryorolling process (rolling at -196°C). In this study, the mentioned alloy was rolled at -196°C to 40% and 70% thickness reduction, and mechanical properties, fatigue life, and fatigue crack growth rate were evaluated using uniaxial tensile tests, constant amplitude fatigue tests, and fatigue crack growth rate tests under decreasing ΔK conditions. In samples reduced by 70% thickness, an ultra-fine-grained structure was observed, and overall, mechanical and fatigue properties in the ultra-fine-grained state increased considerably compared to the base material. In another study in 2011, Panigrahi et al. [12] investigated the tensile and impact properties of Al 7075 alloy reduced by 70% at -196°C. They also examined the effect of heat treatment (short-time annealing and aging) on optimizing the material's properties in tensile testing.

Esmaeili et al. [13] studied the fatigue behavior of Al 7075 alloy after the ECAP process. They plotted the S-N diagrams of the material before and after ECAP, and the results indicated an improvement in fatigue strength in both low-cycle and high-cycle fatigue regimes. The fatigue limit also increased by 59% and 64% after the first and fourth ECAP passes, respectively. Moazam and Honarpishe [14-16] studied the mechanical properties, microstructure and residual stress distribution of Al-7075 alloy processed by cyclic closed die forging. They introduced several methods to implement the cyclic close die forging on Al 7075 alloy. Their results indicated that using CCDF process improves the mechanical properties, decreases the level of the residual stresses, and refines the microstructure of Al 7075 compared with compare with T6 condition.

The main objective of this paper is an experimental investigation of the effect of combining the CCDF process with precipitation hardening heat treatment on the fatigue crack growth rate of aluminum alloy 7075. To this end, samples under different conditions (base T6, T6 with one pass of CCDF, and T6 with two passes of CCDF) were prepared and subjected to fatigue crack growth testing according to the ISO 12108 standard. By accurately measuring crack length during cyclic loading and calculating da/dN as a function of ΔK, the performance of each condition was compared and analyzed.

This research seeks to answer the following questions:

1. Can the CCDF process reduce the fatigue crack growth rate of 7075-T6 alloy?
2. What is the effect of the number of CCDF process passes (one and two passes) on crack growth behavior?
3. What are the potential mechanisms for the improvement in fatigue behavior resulting from the combination of CCDF and precipitation hardening?

The results of this study can provide a basis for developing and optimizing hybrid processes to produce aluminum components with higher fatigue life for critical engineering applications.

2. Research Methodology

The CCDF process die consists of two main parts: the piston and the die. The sample is placed in the die cavity, and the pressure applied by the piston causes the workpiece to deform within the die cavity. The clearance between the piston and the die cavity is of great importance. Insufficient clearance leads to high friction and potential jamming of the piston inside the die, while excessive clearance results in flash formation between the piston and the die. Considering the aforementioned factors and empirical tests, a clearance of 0.05 mm at the front part of the piston was adopted, and the side walls of the piston are tapered with a negative draft angle of 2 degrees from the front toward the rear. The material selected for both the die and piston is tool steel, with their hardness maintained in the range of 48–52 HRC. Fig. 1 shows the geometry of the initial samples in the states before and after the CCDF process.

To evaluate the effect of the CCDF process on the fatigue behavior of aluminum alloy 7075, processed samples after undergoing one and two passes of the CCDF process, as well as precipitation-hardened samples in the T6 condition, were subjected to fatigue crack growth rate testing. In order to create a supersaturated solid solution at room temperature, the following procedure was performed: solution heat treatment at 470±20°C for 2 hours, followed by water quenching and artificial aging at 120±5°C for 12 hours. The CCDF process was carried out immediately after quenching at -60 °C. It was indicated by the authors that implementation of CCDF on Al 7075 at ambient temperature is impossible due to the initiation of the aging process [14-16]. Therefore, based on the aforementioned studies, the quenching process was performed at a temperature of -60 °C. Samples processed by CCDF were also followed by artificial aging at 120±5 °C for 12 hours.

To assess the reproducibility of the results, two samples were prepared for each of the mentioned conditions. It was decided that if the test results for any group showed significant variance, a third sample would be prepared. These tests were conducted according to the ISO 12108 standard [17]. The test results present the

fatigue crack growth rate as a function of the stress intensity factor range at the crack tip, denoted by ΔK. This factor is defined based on Linear Elastic Fracture Mechanics (LEFM) theory [18]. Reporting results based on this criterion indicates the material's resistance to the growth of cracks smaller than the critical size under cyclic loading. In this experiment, a sample containing a pre-crack is subjected to cyclic loading, and the crack length (a) is measured as a function of the number of loading cycles (N). Using the data collected during the test and the relevant equations, the crack growth increment per cycle (da/dN) is determined and expressed in terms of the corresponding stress intensity factor range.

The testing was performed using a GOTECH servo-hydraulic axial fatigue testing machine, shown in Fig. 2. All fixtures were also manufactured based on the sample dimensions and in accordance with the testing standard.

Compact tension (CT) specimens were used for the testing. The specimens were fabricated such that the loading direction during the test was aligned with the direction of the applied press force during the CCDF process. Fig. 3 shows the dimensions of the specimen used. The notch for the fatigue pre-crack was created using wire electrical discharge machining (EDM).

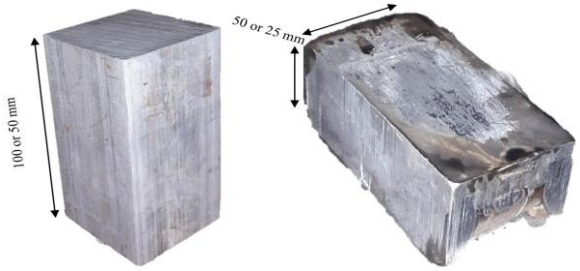

Fig. 1. (a) Initial sample before the CCDF process, (b) sample after performing one pass of the CCDF process.

Fig. 2. Fatigue testing machine used for conducting the fatigue crack growth rate tests.

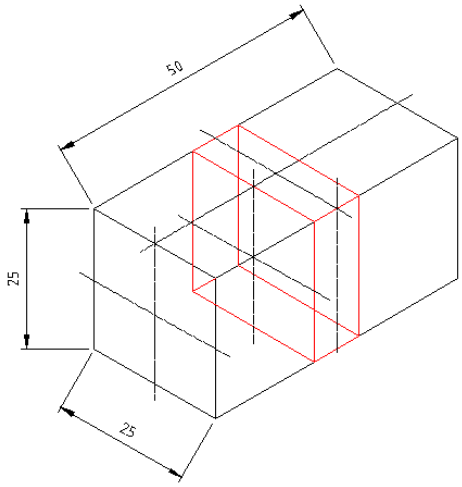

Fig. 3. Geometry and dimensions of the specimen used for the fatigue crack growth rate tests.

The stress intensity factor for the specimen used is calculated using the following equations [14]:

$$K = \frac{F}{BW^{0.5}} g\left(\frac{a}{W}\right) \tag{1}$$

$$g\left(\frac{a}{W}\right) = \frac{(2+\alpha)(0.886 + 4.64\alpha - 13{,}22\alpha^2 + 14{,}72\alpha^3 - 5.6\alpha^4)}{(1-\alpha)^{1/3}} \tag{2}$$

In the above equations, W is the specimen width (16.8 mm), B is the specimen thickness (8 mm), F is the applied force, and α is a coefficient that is determined using the following relation:

$$\alpha = a/W \tag{3}$$

After preparing the specimen and fixture, a fatigue pre-crack is introduced. The purpose of creating a fatigue pre-crack is to prepare a straight, sharp-tipped crack of appropriate length, such that the stress concentration factor from the initial notch is no longer valid at the crack tip. After this stage, the crack growth rate will no longer depend on the load that initiated the crack or its history. To create a fatigue pre-crack, the specimen must be subjected to cyclic loading. For determining the load value in this stage, a load corresponding to 30% to 60% of the KIC value can be used. If a crack does not initiate after 30,000 to 50,000 cycles, the load is increased by 10%. The conditions for creating the fatigue pre-crack in the performed tests are presented in Table 1.

Table 1. Specifications for fatigue pre-cracking

Title	Symbol	Unit	Value
Maximum force	F_max	N	2200
Minimum force	F_min	N	220
Force/stress ratio	R	---	0.1
Loading frequency	f	Hz	10

For the fatigue crack growth rate measurement stage, the increasing stress intensity factor (ΔK) method was employed. In this method, the applied load and stress ratio are held constant. As the crack length increases, the stress intensity factor range (ΔK) correspondingly increases. This value can reach up to the material's fracture toughness. Table 2 presents the specifications for conducting the test during the crack growth rate measurement phase.

Table 2. Loading specifications for the fatigue crack growth rate measurement phase

Title	Symbol	Unit	Value
Maximum force	F_max	N	5500
Minimum force	F_min	N	2750
Force/stress ratio	R	---	0.5
Loading frequency	f	Hz	10

3. Results and Discussion

In this research, the fatigue crack growth rate was used as a criterion to compare the fatigue properties of the material in conditions before and after the combination of precipitation hardening and the CCDF processes. Following the application of cyclic loading, the crack growth was monitored using an optical method with a measurement accuracy of 0.01 mm. According to the ISO 12108 standard, the method used for measuring crack length must have an accuracy better than 0.002W (approximately 0.0336 mm in this case). Fig. 4 shows the setup for measuring fatigue crack growth during the test.

The first indication of fatigue crack initiation in the AA 7075 T6 specimen was observed 54 minutes after the start of the pre-cracking process, and its length reached 3.5 mm after 93 minutes. Similar conditions were achieved for the specimen processed with one pass of CCDF at 72 and 113 minutes after the start of the process. For the specimen processed with two passes of CCDF, the mentioned conditions were achieved after 73 and 115 minutes from the start of the process. These results pertain to the first series of experiments conducted. Fig. 5 shows the condition of the specimen after pre-cracking and before loading for measuring the fatigue crack growth rate.

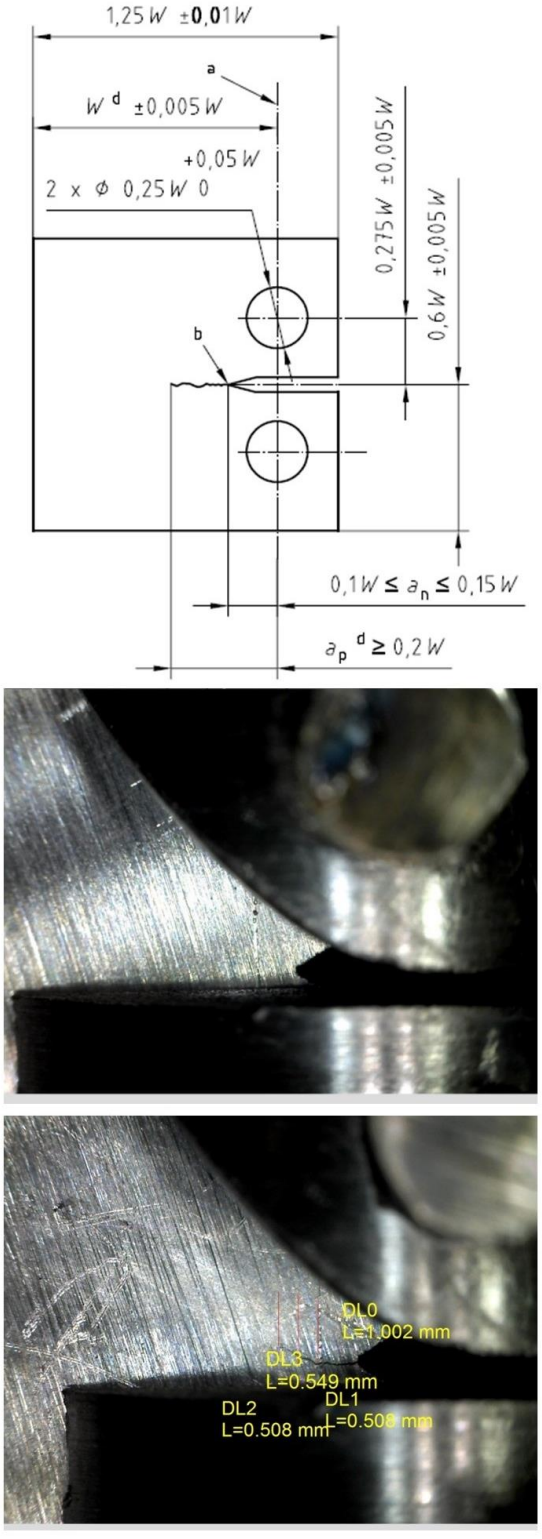

Fig. 4. Measurement of fatigue crack length during the test (schematic of the specimen [17], notch tip without a fatigue crack and propagation of the fatigue crack from the notch tip).

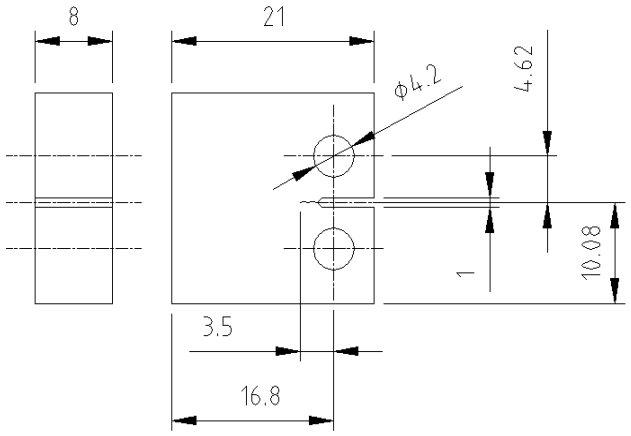

Fig. 5. Photograph of a CT specimen after fatigue pre-cracking (3.5 mm=1.68 mm distance from the notch tip to the hole center+1.82 mm fatigue pre-crack).

The quantitative results related to the pre-cracking stage are presented in Table 3. Given the identical forces and loading conditions, it is evident that the CCDF-processed specimen exhibited greater resistance to fatigue crack initiation. It is also observed that there is no significant difference between the specimens processed by the CCDF method with one pass and two passes.

Table 3. Results of the fatigue pre-cracking stage

Sample type	Test no.	Number of cycles to crack initiation	Number of cycles to reach crack length of 1.82 mm
AA7075 T6	1	32414	55822
1-Pass CCDF	1	43208	67819
2-Pass CCDF	1	43825	69130
AA7075 T6	2	31560	56030
1-Pass CCDF	2	44561	66431
2-Pass CCDF	2	42588	69389

To compare the material resistance to fatigue crack growth under different conditions, an attempt was made to measure the number of loading cycles for the same amount of crack extension across all specimens. Each measurement was taken after every 0.5 mm of fatigue crack extension. The results obtained from the experiments conducted are presented in Tables 4 to 9. According to the ISO 12108 guideline, fatigue crack length (afat) is measured from the tip of the notch. The total length of the crack (a) is defined as the distance from the crack tip to the center of the loading holes. The first measurement was taken at a distance of 2 mm from the notch tip and the values obtained in the first row are used to calculate the crack growth rate in subsequent measurements.

It is worth noting that all tests were continued until the specimen fractured. Based on the results, it is clearly evident that the specimens processed by the CCDF method tolerated at least 1 mm greater fatigue crack growth compared to the T6 specimen. The ΔK (MPa$\sqrt{m}$) for the Al 7075-T6 specimen was 19.95 (MPa$\sqrt{m}$), reaching 23.56 (MPa$\sqrt{m}$) after two CCDF passes. In other words, the tolerance to crack growth under identical loading conditions improved by approximately 18% in the CCDF-processed specimens. Figs. 6, 7, and 8 display the fatigue crack growth rate test results.

The results indicate a higher crack growth rate per loading cycle for the T6 specimen compared to the CCDF-processed specimens. These results demonstrate that at a constant ΔK, the fatigue crack growth rate is lower in the CCDF-processed specimens. It was also observed that the results for specimens processed with one and two passes of the CCDF process are very similar, with no significant difference between them. To better understand the results, the combination of the both test series is presented in Fig. 8.

Table 4. Fatigue crack growth rate test results for the AL 7075-T6 specimen (Test 1)

No.	afat (mm)	N (cycles)	a (mm)	a(j) avg. (mm)	g(a/W)	ΔK (MPa$\sqrt{m}$)	da/dN (mm/cycle)
1	2	2350	3.68				
2	2.5	4203	4.18	3.93	4.711643	12.4957	0.000269833
3	3	5329	4.68	4.43	5.109715	13.55142	0.00044405
4	3.5	6092	5.18	4.93	5.526195	14.65596	0.000655308
5	4	6474	5.68	5.43	5.967392	15.82605	0.001308901
6	4.5	6762	6.18	5.93	6.440967	17.08202	0.001736111
7	5	7010	6.68	6.43	6.956285	18.44869	0.002016129
8	5.5	7205	7.18	6.93	7.524868	19.95662	0.002564103

Table 5. Fatigue crack growth rate test results for the AL 7075-T6 specimen (Test 2)

No.	afat (mm)	N (cycles)	a (mm)	a(j)avg. (mm)	g(a/W)	ΔK (MPa√m)	da/dN (mm/cycle
1	2	2466	3.68				
2	2.5	4410	4.18	3.93	4.711643	12.4957	0.000257202
3	3	5593	4.68	4.43	5.109715	13.55142	0.000422654
4	3.5	6397	5.18	4.93	5.526195	14.65596	0.000621891
5	4	6793	5.68	5.43	5.967392	15.82605	0.001262626
6	4.5	7102	6.18	5.93	6.440967	17.08202	0.001618123
7	5	7361	6.68	6.43	6.956285	18.44869	0.001930502
8	5.5	7564	7.18	6.93	7.524868	19.95662	0.002463054

Table 6. Fatigue crack growth rate test results for the specimen processed with one pass of the CCDF process (Test 1)

No.	afat (mm)	N (cycles)	a (mm)	a(j)avg. (mm)	g(a/W)	ΔK (MPa√m)	da/dN (mm/cycle
1	2	3180	3.68				
2	2.5	6210	4.18	3.93	4.711643	12.4957	0.000165017
3	3	7714	4.68	4.43	5.109715	13.55142	0.000332447
4	3.5	8664	5.18	4.93	5.526195	14.65596	0.000526316
5	4	9206	5.68	5.43	5.967392	15.82605	0.000922509
6	4.5	9548	6.18	5.93	6.440967	17.08202	0.001461988
7	5	9835	6.68	6.43	6.956285	18.44869	0.00174216
8	5.5	9993	7.18	6.93	7.524868	19.95662	0.003164557
9	6	10121	7.68	7.43	8.16101	21.64372	0.00390625
10	6.5	10243	8.18	7.93	8.882625	23.55751	0.004098361

Table 7. Fatigue crack growth rate test results for the specimen e processed with one pass of the CCDF process (Test 2)

No.	afat (mm)	N (cycles)	a (mm)	a(j)avg. (mm)	g(a/W)	ΔK (MPa√m)	da/dN (mm/cycle
1	2	3274	3.68				
2	2.5	6394	4.18	3.93	4.711643	12.4957	0.000160256
3	3	7947	4.68	4.43	5.109715	13.55142	0.000321958
4	3.5	8922	5.18	4.93	5.526195	14.65596	0.000512821
5	4	9485	5.68	5.43	5.967392	15.82605	0.000888099
6	4.5	9831	6.18	5.93	6.440967	17.08202	0.001445087
7	5	10132	6.68	6.43	6.956285	18.44869	0.00166113
8	5.5	10293	7.18	6.93	7.524868	19.95662	0.00310559
9	6	10425	7.68	7.43	8.16101	21.64372	0.003787879
10	6.5	10550	8.18	7.93	8.882625	23.55751	0.004

Table 8. Fatigue crack growth rate test results for the specimen processed with two passes of the CCDF process (Test 1)

No.	afat (mm)	N (cycles)	a (mm)	a(j)avg. (mm)	g(a/W)	ΔK (MPa√m)	da/dN (mm/cycle
1	2	3312	3.68				
2	2.5	6471	4.18	3.93	4.711643	12.4957	0.000158278
3	3	8044	4.68	4.43	5.109715	13.55142	0.000317864
4	3.5	9028	5.18	4.93	5.526195	14.65596	0.00050813
5	4	9596	5.68	5.43	5.967392	15.82605	0.000880282
6	4.5	9947	6.18	5.93	6.440967	17.08202	0.001424501
7	5	10255	6.68	6.43	6.956285	18.44869	0.001623377
8	5.5	10417	7.18	6.93	7.524868	19.95662	0.00308642
9	6	10550	7.68	7.43	8.16101	21.64372	0.003759398
10	6.5	10674	8.18	7.93	8.882625	23.55751	0.004032258

Table 9. Fatigue crack growth rate test results for the specimen processed with two passes of the CCDF process (Test 2)

No.	afat (mm)	N (cycles)	a (mm)	a(j)avg. (mm)	g(a/W)	ΔK (MPa√m)	da/dN (mm/cycle
1	2	3543	3.68				
2	2.5	6922	4.18	3.93	4.711643	12.4957	0.000147973
3	3	8601	4.68	4.43	5.109715	13.55142	0.000297796
4	3.5	9658	5.18	4.93	5.526195	14.65596	0.000473037
5	4	10266	5.68	5.43	5.967392	15.82605	0.000822368
6	4.5	10640	6.18	5.93	6.440967	17.08202	0.001336898
7	5	10974	6.68	6.43	6.956285	18.44869	0.001497006
8	5.5	11149	7.18	6.93	7.524868	19.95662	0.002857143
9	6	11286	7.68	7.43	8.16101	21.64372	0.003649635
10	6.5	11420	8.18	7.93	8.882625	23.55751	0.003731343

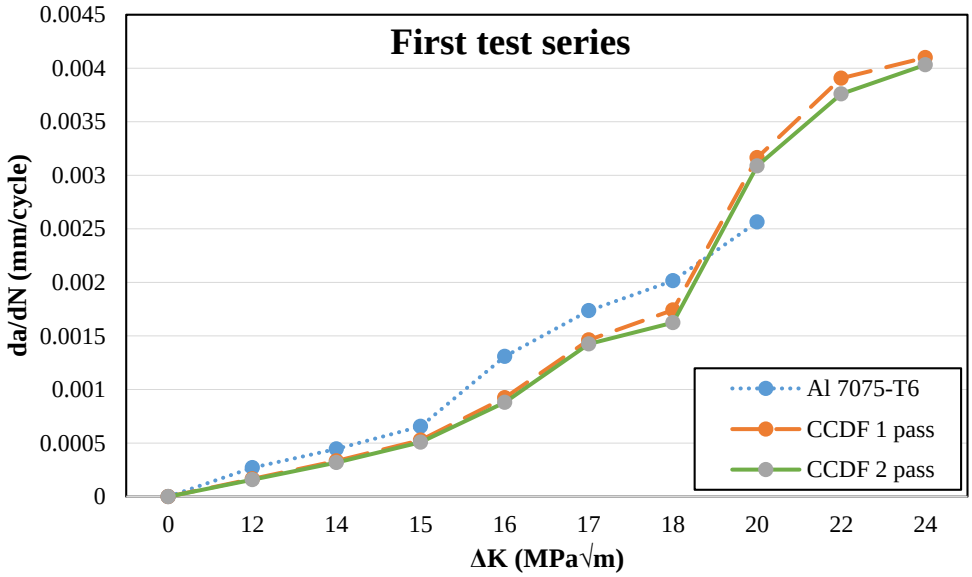

Fig. 6. Fatigue crack growth rate test results for different specimens (First test series).

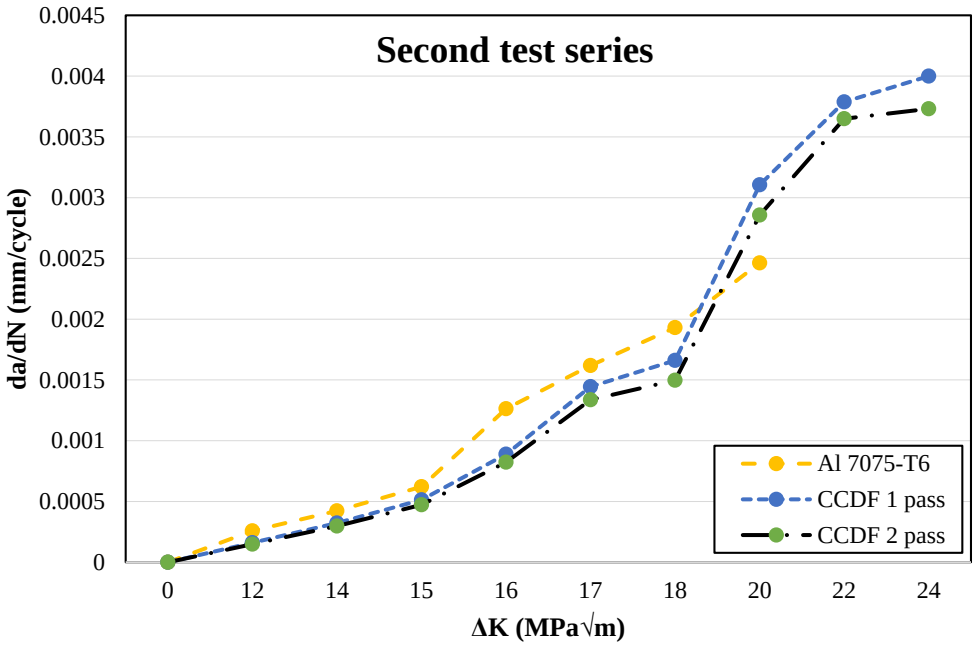

Fig. 7. Fatigue crack growth rate test results for different specimens (Second test series).

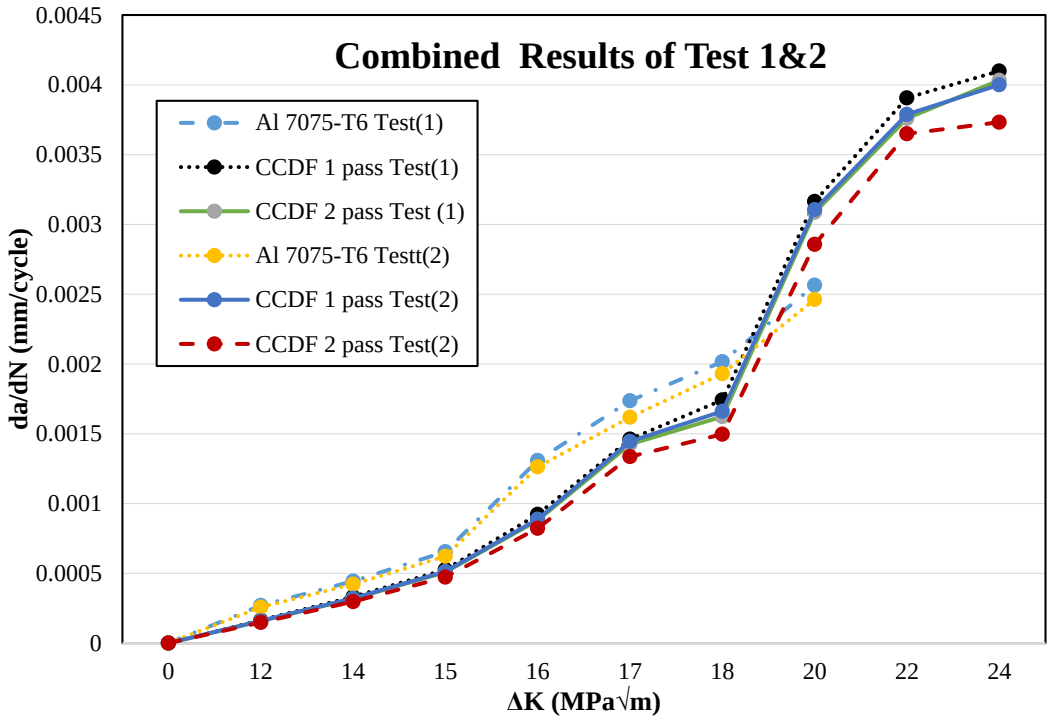

Fig. 8. Fatigue crack growth rate test results for different specimens (Combined results).

4. Conclusion

In this research, the effect of the CCDF process on the fatigue crack growth behavior of aluminum alloy 7075 was experimentally investigated. The most important findings are as follows:

- CCDF-processed specimens (both one-pass and two-pass) exhibited higher resistance to fatigue crack initiation compared to the base T6 condition, as confirmed by the increased number of loading cycles to crack initiation.
- Specimens processed by the CCDF method tolerated over 1 mm more fatigue crack growth compared to the T6 specimen.
- The ΔK (MPa√m) for the Al 7075-T6 specimen was 19.95 MPa√m and reached 23.56 MPa√m after running two CCDF passes
- The fatigue crack growth rate (da/dN) in CCDF-processed specimens was, on average, 18% lower than that of the T6 specimen at the same ΔK value, indicating a significant improvement in crack growth tolerance.
- No significant difference was observed between the performance of one-pass and two-pass CCDF specimens, suggesting that a single pass of this process is sufficient to achieve the desired improvements in fatigue behavior.
- These improvements are primarily attributed to microstructural refinement, grain size reduction, and optimized precipitate distribution resulting from the CCDF process.

These results demonstrate that combining the CCDF process with precipitation hardening heat treatment is an effective strategy for developing aluminum alloys with higher fatigue life, suitable for cyclic loading applications in advanced industries. It is recommended that future research focus on the effects of CCDF process parameters (such as forging temperature and strain rate) and conduct more in-depth microstructural investigations (e.g., TEM, EBSD) to better understand the underlying mechanisms.

Author's contributions

M. A. Moazam: Conceptualization, Methodology, Formal analysis, Investigation, Data curation, Writing - review & editing

M. Honarpisheh: Conceptualization, Methodology, Formal analysis, Investigation, Data curation, Writing - original draft, Writing - review & editing

Competing interests

The authors have no competing interests to declare that are relevant to the content of this article.

Funding

The authors declare that no funds, grants, or other support were received during the preparation of this manuscript.

5. References

[1] Gosh A. K. (1988). *Method of producing a fine grain aluminum alloy using three axes deformation*. U.S. Patent No. 4721537.

[2] Cherukuri, B., Srinivasan, R. (2006). Properties of AA6061 processed by multi-axial compressions/forging (MAC/F). *Materials and Manufacturing Processes*, *21*(5), 519-525. https://doi.org/10.1080/10426910500471649

[3] Zude, Z., Qiang, C., Zejun, T., Chuankai, H. (2010). Microstructural evolution and tensile mechanical properties of AM60B magnesium alloy prepared by the SIMA route. *Journal of Alloys and Compounds*, *497*, 402–411. https://doi.org/10.1016/S1003-6326(13)62853-8

[4] Gao-zhan, Z., Lin, Y., Xun-xing, D., Xiao-hua, R., Li-min, Z., Ting-jun, Y., Xiang-yong, G., Shao-nan. H. (2012). Microstructure evolution and mechanical properties of AZ80 alloy reheated from as-cast and deformed states, *Transactions of Nonferrous Metals Society of China*, *22*(2), 450-456. https://doi.org/10.1016/S1003-6326(12)61745-2

[5] Xia, X., Huang, J., Zhang, R., Zhao, Q., Hu, Q., Deng, T., Xiao, Y. Sun, J. (2013). Evolution of microstructure and mechanical properties of AZ61 Mg alloy during cyclic closed die forging. *Materials Research Innovations 17*(1), 130-134. https://doi.org/10.1179/1432891713Z.000000000203

[6] Metayer, J., Bing, Y., Wei, G., Qu-dong, W., Hao, Z., Mollet, F. (2014). Microstructure and mechanical properties of Mg–Si alloys processed by cyclic closed-die forging, *Transactions of Nonferrous Metals Society of China*, *24*(1), 66-75. https://doi.org/10.1016/S1003-6326(14)63029-6

[7] Valiev, R. Z., Islamgaliev, R. K., & Alexandrov, I. V. (2000). Bulk nanostructured materials from severe plastic deformation. *Progress in materials science*, *45*(2), 103-189. https://doi.org/10.1016/S0079-6425(99)00007-9

[8] Estrin, Y., & Vinogradov, A. (2013). Extreme grain refinement by severe plastic deformation: A wealth of challenging science. *Acta Materialia*, *61*(3), 782-817. https://doi.org/10.1016/j.actamat.2012.10.038

[9] Heinz, A., Haszler, A., Keidel, C., Moldenhauer, S., Benedictus, R., & Miller, W. S. (2000). Recent development in aluminium alloys for aerospace applications. *Materials Science and Engineering: A*, *280*(1), 102-107. https://doi.org/10.1016/S0921-5093(99)00674-7

[10] Williams, J. C., & Starke, E. A. (2003). Progress in structural materials for aerospace systems. *Acta Materialia*, *51*(19), 5775-5799. https://doi.org/10.1016/j.actamat.2003.08.023

[11] Sha, G., & Cerezo, A. (2004). Early-stage precipitation in Al–Zn–Mg–Cu alloy (7050). *Acta Materialia*, *52*(15), 4503–4516. https://doi.org/10.1016/j.actamat.2004.06.025

[12] Panigrahi, S. K., & Jayaganthan, R. (2011). Development of ultrafine grained high strength age hardenable Al 7075 alloy by cryorolling. *Materials & Design*, *32*(6), 3150-3160. https://doi.org/10.1016/j.matdes.2011.02.051

[13] Esmaeili, A., Shaeri, H., Noghani, M., Razaghian, A. (2018). Fatigue behavior of AA7075 aluminium alloy severely deformed by equal channel angular pressing. *Journal of Alloys and Compounds*, *757*, 324-332. https://doi.org/10.1016/j.jallcom.2018.05.085

[14] Moazam, M. A., & Honarpisheh, M. (2019). Ring-core integral method to measurement residual stress distribution of Al-7075 alloy processed by cyclic close die forging. *Materials Research Express*, *6*(8), 0865j3. https://iopscience.iop.org/article/10.1088/2053-1591/ab29b6

[15] Moazam, M. A., & Honarpisheh, M. (2020). The effects of combined cyclic close die forging and aging process on microstructure and mechanical properties of AA7075. *Proceedings of the Institution of Mechanical Engineers, Part L: Journal of Materials: Design and Applications*, *234*(9), 1242-1251. https://doi.org/10.1177/1464420720931528

[16] Moazam, M. A., & Honarpisheh, M. (2021). Improving the mechanical properties and reducing the residual stresses of AA7075 by combination of cyclic close die forging and precipitation hardening. *Proceedings of the Institution of Mechanical Engineers, Part L: Journal of Materials: Design and Applications*, *235*(3), 542-549. https://doi.org/10.1177/1464420720972428

[17] ISO 12108:2018. (2018). *Metallic materials — Fatigue testing — Fatigue crack growth method*. International Organization for Standardization.

[18] ASTM E647-15. (2015). *Standard test method for measurement of fatigue crack growth rates*. ASTM International.